

Diffusivity fractionations of H₂¹⁶O/H₂¹⁷O and H₂¹⁶O/H₂¹⁸O in air and their implications for isotope hydrology[†]

Eugeni Barkan* and Boaz Luz

The Institute of Earth Sciences, The Hebrew University of Jerusalem, Givat Ram, Jerusalem 91904, Israel

Received 22 May 2007; Revised 8 July 2007; Accepted 12 July 2007

We have determined the isotope effects of ¹⁷O and ¹⁸O substitution of ¹⁶O in H₂O on molecular diffusivities of water vapor in air by the use of evaporation experiments. The derived diffusion fractionation coefficients ¹⁷α_{diff} and ¹⁸α_{diff} are 1.0146 ± 0.0002 and 1.0283 ± 0.0003, respectively. We also determined, for the first time, the ratio ln(¹⁷α_{diff})/ln(¹⁸α_{diff}) as 0.5185 ± 0.0002. This ratio, which is in excellent agreement with the theoretical value of 0.5184, is significantly smaller than the ratio in vapor-liquid equilibrium (0.529). We show how this new experimental information gives rise to ¹⁷O excess in meteoric water, and how it can be applied in isotope hydrology. Copyright © 2007 John Wiley & Sons, Ltd.

For more than four decades, water isotope ratios (HD¹⁶O/H₂¹⁶O and H₂¹⁸O/H₂¹⁶O) have played a key role in understanding the hydrologic cycle. The combination of the three isotope species adds information on evaporation conditions because the isotope fractionations are different in the processes of liquid-vapor equilibrium and in vapor diffusion in air (e.g. Gat¹).

Luz and Barkan² were the first to demonstrate that fractionations among the three oxygen isotopes were different in evaporation than in previously studied processes in meteoric waters.³ Confirmation of this observation came from a global budget of factors affecting atmospheric oxygen,⁴ and these findings led to the suggestion that ¹⁷O/¹⁶O and ¹⁸O/¹⁶O ratios in liquid water and ice may yield additional information on processes of evaporation and condensation of water vapor.⁵ It was clear, however, that realization of the potential of ¹⁷O/¹⁶O and ¹⁸O/¹⁶O ratios in water requires the development of a high-precision analytical method for isotopic analyses of water. Such a method, based on the fluorination of water with CoF₃, was developed by us, and used to measure fractionations in liquid-vapor equilibria.⁶ Direct experimental determination of the fractionation due to vapor diffusion in air was, however, lacking. This posed a serious limitation on our ability to constrain hydrologic systems where water vapor is involved. Therefore, we initiated the present study and have measured the fractionation occurring in vapor diffusion in air with very high precision.

*Correspondence to: E. Barkan, Institute of Earth Sciences, The Hebrew University of Jerusalem, Givat Ram, Jerusalem 91904, Israel.

E-mail: eugenib@cc.huji.ac.il

Contract/grant sponsor: The Israel Science Foundation; contract/grant number: 188/03-13.0.

[†]This article was published online on 20 Aug 2007. Errors were subsequently identified and corrected by an erratum notice that was published online only on 24 Aug 2007; DOI: 10.1002/rcm.3233. This printed version incorporates the amendments identified by the erratum notice.

EXPERIMENTAL

Theoretical background

Throughout the present study we presented the fractionation factors (α) such that they are greater than 1. Thus, the oxygen water fractionation factor between an evaporating flux (E) and a liquid water surface (W) is defined as: α_{evap} = R_W/R_E (and not R_E/R_W), where R_W and R_E are the isotopic ratios (H₂¹⁷O/H₂¹⁶O or H₂¹⁸O/H₂¹⁶O) of liquid and evaporating water, respectively. In the case of vapor flux from an evaporating water reservoir at steady state, this ratio can be expressed as:^{7–9}

$$\alpha_{\text{evap}} = R_W/R_E = \frac{\alpha_{\text{diff}}\alpha_{\text{eq}}(1-h)}{1-\alpha_{\text{eq}}h(R_A/R_W)} \quad (1)$$

where α_{eq} is the liquid-vapor equilibrium fractionation factor; R_A is the isotopic ratio of air moisture, and h is relative air humidity. α_{diff} is the diffusion fractionation factor and is expressed as (D_L/D_H)ⁿ, where D_H and D_L are the molecular diffusivities of water including heavy (H, ¹⁷O or ¹⁸O) and light (L, ¹⁶O) isotopes, respectively. The exponent n depends on the ratio of turbulent to molecular diffusion and equals 1 when the turbulence is zero.

In our experimental setup the only source of water vapor to the air column overlying the liquid is the flux of evaporating water vapor, hence R_A = R_E and α_{evap} = R_W/R_A. In this case, Eqn. (1) can be rewritten to express α_{diff} as:

$$\alpha_{\text{diff}} = \frac{\alpha_{\text{evap}}/\alpha_{\text{eq}} - h}{1-h} \quad (2)$$

where all the parameters on the right are either known or can be determined experimentally. α_{evap} can be obtained from Rayleigh fractionation experiments, and the relative humidity (h) is calculated from the ratio of the evaporative flux to the rate of dry air flow. ¹⁸α_{eq} is known from previous

experimental work.^{6,10,11} Finally, because in the triple isotope system the fractionation factors are related by the exponent θ (e.g. Mook¹²):

$$\theta = \frac{\ln^{17}\alpha}{\ln^{18}\alpha} \quad (3)$$

we can calculate $^{17}\alpha_{\text{eq}}$ from the relation $^{17}\alpha_{\text{eq}} = (^{18}\alpha_{\text{eq}})^\theta$, where the exponent θ equals 0.529 as measured in our previous work.⁶ For the case of fractionation due to diffusion, Eqn. (3) becomes:

$$\theta_{\text{diff}} = \frac{\ln(^{17}\alpha_{\text{diff}})}{\ln(^{18}\alpha_{\text{diff}})} = \frac{\ln((^{16}\text{D}/^{17}\text{D})^n)}{\ln((^{16}\text{D}/^{18}\text{D})^n)} = \frac{\ln(^{16}\text{D}/^{17}\text{D})}{\ln(^{16}\text{D}/^{18}\text{D})} \quad (4)$$

As can be seen, θ_{diff} is independent of the turbulence transport component.

Experimental setup

In our design we followed the approach of previous studies,^{7,9,13} whereby the isotope effects of diffusion were determined from Rayleigh distillation experiments in which the flux of evaporating water was removed into a stream of air. In these experiments it was shown that the diffusion fractionation factors for $\text{HD}^{16}\text{O}/\text{H}_2^{16}\text{O}$ and $\text{H}_2^{18}\text{O}/\text{H}_2^{16}\text{O}$ remained constant over a wide range (5–95%) of relative humidity of the overlying air. Furthermore, as expected from Eqn. (1), and also shown experimentally, the magnitude of measured α_{evap} becomes smaller as the relative humidity and

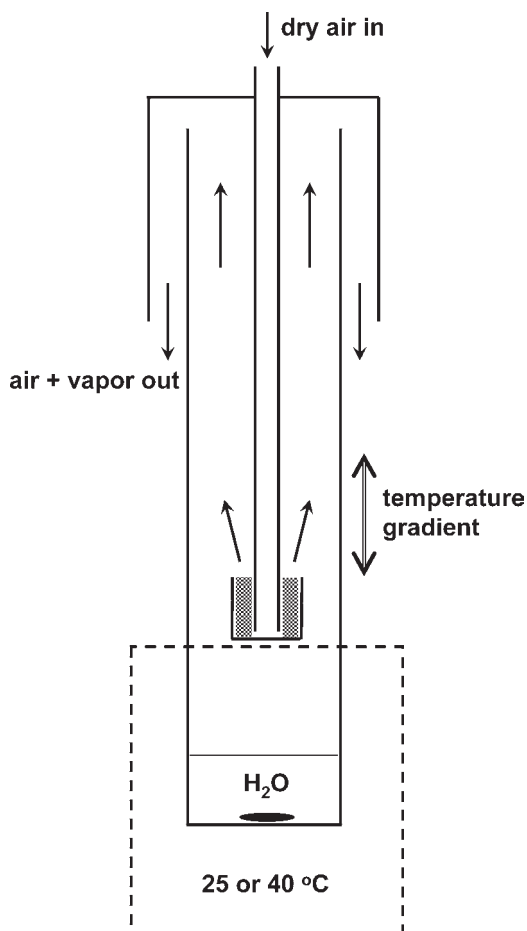


Figure 1. Schematic illustration of the evaporation apparatus (not to scale).

turbulence increase. Therefore, in order to maximize the isotope effects of molecular diffusion, and thus to minimize errors, we attempted to diminish air turbulence while keeping the relative humidity close to zero.

A schematic illustration of the experimental setup is shown in Fig. 1. It consists of a glass test tube with a cross-section of $\sim 1 \text{ cm}^2$ and a Teflon-coated stir bar at the bottom. The lower part ($\sim 3.5 \text{ cm}$) of the tube is kept at constant temperature. A stream of dry air (200 mL/min) flows through a 2 mm i.d. stainless steel tube. The bottom part of this tube is inserted into a small thimble containing glass wool that directs a smoothed upwards flow of dry air away from the water-air interface. The upper part of the test tube is heated ($\sim 65^\circ\text{C}$) and a temperature gradient is generated between the thermostatic lower part and the heated upper part.

An amount (between 0.5 and $1.5 \pm 0.001 \text{ g}$) of distilled water of known $\delta^{17}\text{O}$ and $\delta^{18}\text{O}$ was injected with a syringe to the bottom of the tube before each experimental run. During the run the water was gently stirred in order to minimize the formation of a cooled surface layer. Depending on the temperature of the water and the humidity gradient in the air column above it, the evaporation rate was about 8.3 and $4.1 \text{ g m}^{-2} \text{ s}^{-1}$ at 40 and 25°C , respectively. Accordingly, the relative humidity of the out-flowing air-stream was calculated as 0.0135 and 0.0067%. The water at the end of each experiment was weighed in order to determine the remaining fraction, and then transferred to a glass vial for further preparation in an automatic fluorination line (see details in Barkan and Luz⁶).

It should be mentioned that the above design was developed after preliminary tests that showed that the resulting isotope fractionation was sensitive to whether the air flow was directed towards or away from the water surface, on the presence or absence of diffusing glass wool and on relative humidity. In addition, the heated upper part of the test tube ensured that there was no condensation and no risk of back diffusion of water vapor. Likewise, the thermal gradient minimized turbulence by enhancing density stratification of the air column above the dry air outlet.

Isotope analyses

The analytical method for determination of the oxygen isotopic ratios of water is detailed in Barkan and Luz.⁶ In brief, $2 \mu\text{L}$ of water are converted by fluorination into O_2 gas using CoF_3 reagent. The produced O_2 is transferred to a stainless steel holding tube on a collection manifold immersed in liquid helium. After processing, the manifold is warmed up to room temperature and connected to a Finnigan Delta^{plus} isotope-ratio mass spectrometer (Thermo Scientific, Bremen, Germany). The $\delta^{17}\text{O}$ and $\delta^{18}\text{O}$ of O_2 are measured simultaneously in dual-inlet mode by multi-collector mass spectrometry. Each mass spectrometric measurement consists of three separate runs during which the ratio of sample to reference is determined 30 times. The pressures of the sample and reference gas are balanced before each of the three runs. The reported δ -values are averages of three runs with respect to Vienna Standard Mean Ocean Water (VSMOW). The mass spectrometer errors (standard error of the mean ($n = 90$) multiplied by Student's

t-factor for 95% confidence limits) in $\delta^{18}\text{O}$ and $\delta^{17}\text{O}$ are 0.004 and 0.008‰, respectively.

RESULTS

The experiments were conducted at 25 and 40°C, and the duration of each experiment was adjusted in order to obtain variations in the remaining fraction of liquid water in the range 0.8 to 0.3. We ran triplicates of each sample on the fluorination system and all the results are listed in Table 1.

From these data we first calculated the fractionation coefficient during water evaporation ($^*\alpha_{\text{evap}}$) using the Rayleigh fractionation relationship:

$$^*\alpha_{\text{evap}} = \frac{\ln(^*R_{\text{end}}/^*R_{\text{start}})}{\ln(f)} + 1 \quad (5)$$

where f is the remaining water fraction, and * stands for ¹⁷ or ¹⁸.

To demonstrate our overall analytical performance, we present in Fig. 2 the oxygen-18 enrichments vs. $\ln(f)$ for all the experiments at a given temperature. As can be clearly seen, the correlation is excellent. The obtained values of $^*\alpha_{\text{evap}}$ were then used to calculate $^*\alpha_{\text{diff}}$ with Eqn. (2) and finally θ_{diff} was calculated from $^{17}\alpha_{\text{diff}}$ and $^{18}\alpha_{\text{diff}}$.

The precisions of the presented $^{17}\alpha_{\text{diff}}$, $^{18}\alpha_{\text{diff}}$ and θ_{diff} values are 0.0001, 0.0002 and 0.0001, respectively. The average absolute differences between replicates were around

0.012‰ for $\delta^{17}\text{O}$ and 0.025‰ for $\delta^{18}\text{O}$ while the maximum difference in $\delta^{17}\text{O}$ was about 0.03‰ and 0.05‰ in $\delta^{18}\text{O}$ (Fig. 3). These differences are considerably greater than the mass spectrometer errors, and at the first sight it is not clear how such extremely high precision in θ_{diff} (0.001 or better) can be achieved. However, as has been pointed out in our previous work,¹⁴ the shifts in $\delta^{18}\text{O}$ and $\delta^{17}\text{O}$ within replicates are not independent: when $\delta^{18}\text{O}$ increases, there is a parallel increase, but in general of a smaller magnitude, in $\delta^{17}\text{O}$. Such a result is not surprising because both $\delta^{17}\text{O}$ and $\delta^{18}\text{O}$ are derived from the same water sample prepared to yield O₂ gas, which is then measured on the mass spectrometer. We thus expect that any bias due to sample handling during preparation and measurement will be mass-dependent. In this case, any shift in $\delta^{17}\text{O}$ is expected to be about 0.5 that of $\delta^{18}\text{O}$. As a result, for mass-dependent slopes, which are always close to 0.52, the $\delta^{17}\text{O}$ and $\delta^{18}\text{O}$ errors tend to cancel out and the derived θ_{diff} values are very robust.

The high precision of our θ_{diff} values can be also demonstrated in an additional way, by direct regression of $\delta^{17}\text{O}$ vs. $\delta^{18}\text{O}$ (Fig. 4). The regression slope in the $\ln(\delta^{17}\text{O} + 1)$ vs. $\ln(\delta^{18}\text{O} + 1)$ plots equals $(^{17}\alpha_{\text{evap}} - 1)/(^{18}\alpha_{\text{evap}} - 1)$. The error in this slope depends on all the factors affecting either $^{17}\alpha_{\text{evap}}$ or $^{18}\alpha_{\text{evap}}$ except the remaining fraction (f) because it is identical for both and cancels out. The standard errors of the slopes were 0.0001 and 0.0002 for the experiments at 40 and 25°C, respectively. The excellent goodness of fit is also

Table 1. Remaining fraction (f), $\delta^{17}\text{O}$ and $\delta^{18}\text{O}$ (‰ vs. VSMOW) of water at the end of the evaporation experiments, fractionation factors and their ratios^a

f	Replicate	$\delta^{17}\text{O}$	$\delta^{18}\text{O}$	$^{17}\alpha_{\text{diff}}$	$^{18}\alpha_{\text{diff}}$	$\ln(^{17}\alpha_{\text{diff}})/\ln(^{18}\alpha_{\text{diff}})$
40°C						
0.787	1	1.760	3.309	1.014669	1.028485	0.5185
0.787	2	1.765	3.311	1.014691	1.028494	0.5191
0.787	3	1.754	3.294	1.014643	1.028417	0.5188
0.601	1	6.656	12.656	1.014419	1.027978	0.5188
0.601	2	6.642	12.626	1.014390	1.027916	0.5189
0.601	3	6.652	12.646	1.014411	1.027958	0.5189
0.508	1	9.810	18.699	1.014501	1.028135	0.5189
0.508	2	9.822	18.725	1.014519	1.028175	0.5188
0.508	3	9.835	18.751	1.014539	1.028216	0.5187
0.416	1	13.529	25.863	1.014507	1.028165	0.5185
0.416	2	13.544	25.885	1.014525	1.028191	0.5187
0.416	3	13.553	25.905	1.014535	1.028215	0.5186
0.330	1	17.642	33.801	1.014312	1.027782	0.5186
0.330	2	17.657	33.822	1.014326	1.027802	0.5187
0.330	3	17.656	33.834	1.014325	1.027813	0.5185
Regress^b				1.014425 ± 0.00005	1.027998 ± 0.0001	0.5187 ± 0.0001
25°C						
0.797	1	1.641	3.077	1.014487	1.028134	0.5184
0.797	2	1.637	3.066	1.014468	1.028082	0.5187
0.797	3	1.644	3.085	1.014500	1.028172	0.5182
0.508	1	10.410	19.834	1.014703	1.028538	0.5187
0.508	2	10.393	19.801	1.014678	1.028487	0.5188
0.508	3	10.395	19.815	1.014681	1.028509	0.5185
0.308	1	20.200	38.747	1.014714	1.028596	0.5181
0.308	2	20.220	38.778	1.014731	1.028623	0.5182
0.308	3	20.236	38.819	1.014745	1.028659	0.5180
Regress^b				1.014713 ± 0.00005	1.028585 ± 0.0001	0.5183 ± 0.0001

^a All experimental runs were started from the same batch of water, whose isotopic composition was analyzed throughout the duration of the study, and the average values were: $\delta^{17}\text{O} = -2.677 \pm 0.015$, $\delta^{18}\text{O} = -5.133 \pm 0.027$, ^{17}O -excess = 37 ± 4 per meg ($n = 21$).

^b The values and their errors were derived by regression analysis of all the data using the Isoplot 3.00 software,²⁷ which yielded $^{17}\alpha_{\text{evap}}$ and $^{18}\alpha_{\text{evap}}$. Then by using Eqn. (2), we calculated $^{17}\alpha_{\text{diff}}$ and $^{18}\alpha_{\text{diff}}$.

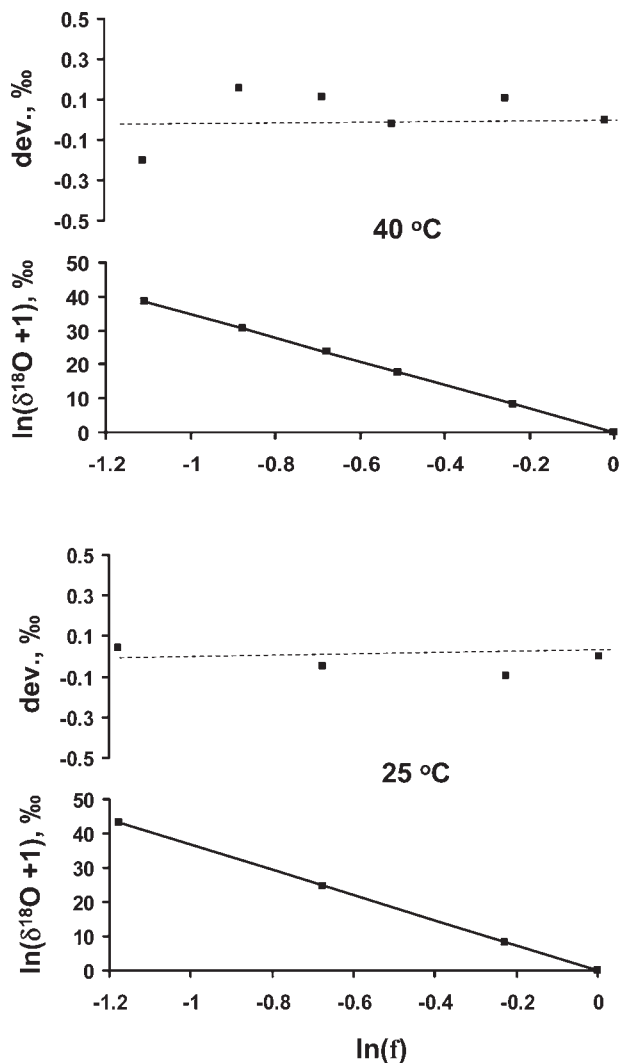


Figure 2. ^{18}O enrichment vs. $\ln(f)$ in the evaporation experiments (lower panels) and deviations from the regression lines (upper panels).

verified by the very small deviations of the points from the regression lines, as can be seen in Fig. 4.

In a recent study⁹ it was stated that evaporative heat loss can result in water-surface cooling of up to 5°C with respect

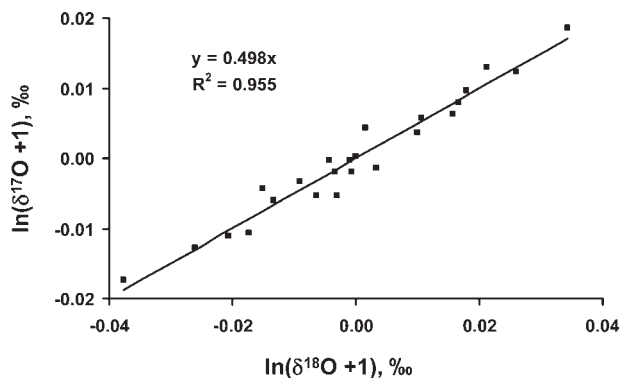


Figure 3. Deviations from the mean ($n = 3$) of replicate fluorinations of all the water samples. For each sample we have three fluorinations (see Table 1) and three points on the plot. Note the mass dependence (slope of ~ 0.5) of the errors in $\ln(\delta^{17}\text{O} + 1)$ vs. $\ln(\delta^{18}\text{O} + 1)$.

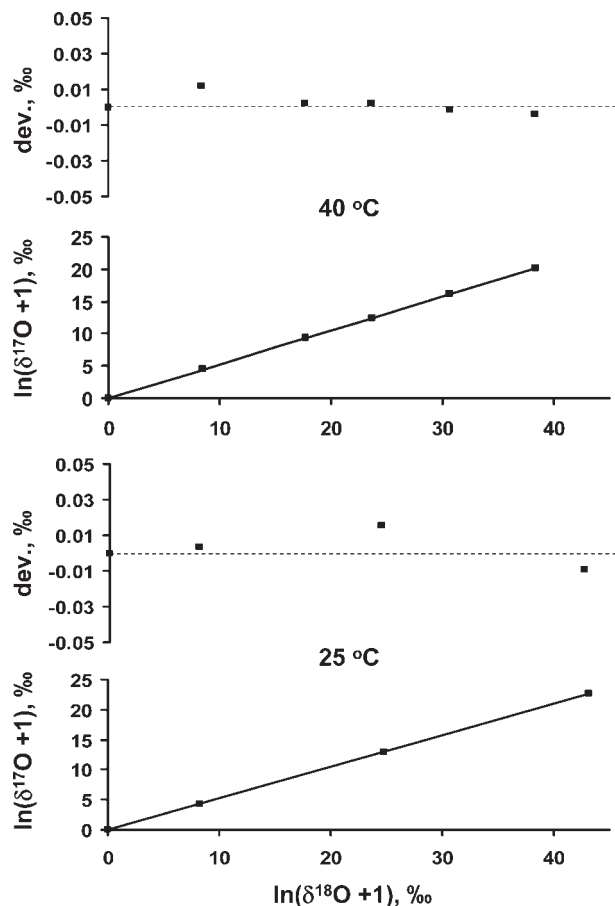


Figure 4. Plots of $\ln(\delta^{17}\text{O} + 1)$ vs. $\ln(\delta^{18}\text{O} + 1)$ in the evaporation experiments (lower panels) and deviations from the regression lines (upper panels).

to the bulk temperature of the liquid. These estimates were based on a calculation using data from Fang and Ward.¹⁵ However, direct measurements¹⁶ of surface cooling under similar experimental conditions as in the above study⁹ showed that the surface-cooling effect should not be greater than 2°C. We argue that in our experimental setup surface cooling was even smaller due to the low evaporation rate and because the liquid was stirred. However, even with 5°C cooling, the effect on $^{18}\alpha_{\text{diff}}$ is only 0.0004, which is of the same order as our experimental precision. Moreover, such a cooling effect on θ_{diff} is 0.0001, which again is similar to our experimental precision.

The results for α_{diff} and θ_{diff} in Table 1 show very slight but significant temperature dependence. However, much additional work involving a very high precision experimental study is necessary in order to verify this observation. For this reason, in the following discussion we will use averaged values for 25 and 40°C: $^{17}\alpha_{\text{diff}} = 1.0146 \pm 0.0002$; $^{18}\alpha_{\text{diff}} = 1.0283 \pm 0.0003$; $\theta_{\text{diff}} = 0.5185 \pm 0.0002$. The obtained average figure for $^{18}\alpha_{\text{diff}}$ is in excellent agreement with the corresponding values of Merlivat¹³ and Mook,¹² 1.0285 ± 0.0007 and 1.0280 ± 0.0005 , respectively. We can thus conclude that our value of $^{17}\alpha_{\text{diff}}$ is also very reliable. To the best of our knowledge no experimental determinations of θ_{diff} have been carried out previously. Angert *et al.*⁵ derived

an estimate of θ_{diff} of 0.511, which is based on a global budget of the three oxygen isotopes in atmospheric O₂, marine photosynthesis, terrestrial photosynthesis and transpiration effects in leaf water. Considering the uncertainties and assumptions involved in their global calculation, it is clear that the 0.511 value is less accurate than our directly derived experimental figure – 0.5185.

From the kinetic theory of gases (e.g. Marrero and Mason¹⁷) we know that:

$$\frac{D_L}{D_H} = \left(\frac{M_H(M_L + M_G)}{M_L(M_H + M_G)} \right)^{1/2} \left(\frac{\Gamma_H + \Gamma_G}{\Gamma_L + \Gamma_G} \right)^2 \quad (6)$$

where M is molecular mass; subscripts L and H stand for the light and heavy isotopes, respectively; subscript G refers to the gas in which the water vapor diffuses (air in our case); and Γ stands for the molecular collision diameters. Assuming that the collision diameters for the different isotope species are identical (Hirshfelder *et al.*¹⁸), we calculate the ratio ¹⁶D/¹⁸D as 1.0323, which is larger than our and other^{12,13} experimentally determined values of ¹⁸ α_{diff} .

We can think of three possible ways to explain the discrepancy between the experimental results and the calculated value. First, recalling that ¹⁸ $\alpha_{\text{diff}} = (^{16}\text{D}/^{18}\text{D})^n$, we can explain the difference by letting n be ~0.88 instead of 1, or in other words suggest that we, as well as others,^{12,13} did not manage to completely eliminate turbulence. However, Merlivat¹³ very carefully tested that turbulence was practically zero in her experiments. Consequently, she suggested a second possibility that the collision diameter of H₂¹⁸O is slightly smaller than that of H₂¹⁶O thus giving rise to larger diffusivity of the heavy molecule. More recently, Cappa *et al.*⁹ argued that such different diameters are unlikely. A third alternative, proposed by Mook,¹² is that molecular clustering in the vapor phase increases the effective molecular masses. Water dimers (H₂O–H₂O pairs) are the main form of such clusters in air,¹⁹ and a simple calculation shows that the discrepancy is resolved if water dimers consist of about ~20% of air moisture. This amount, however, is two orders of magnitude larger than the concentration of water dimers in air.²⁰

We do not have a satisfactory explanation for the difference between simple theory and the observed ¹⁸ α_{diff} and recommend that more theoretical studies are needed in order to resolve this problem. We note, however, that our experimentally derived θ_{diff} (0.5185 ± 0.0003) is in nearly perfect agreement with the theoretical value (0.5184) calculated with the assumption that the collision diameters of H₂¹⁶O, H₂¹⁷O and H₂¹⁸O are identical.

IMPLICATIONS FOR ISOTOPE HYDROLOGY

Generally, in studies of water isotopes, variations in the ratios H₂¹⁷O/H₂¹⁶O, H₂¹⁸O/H₂¹⁶O and HD¹⁶O/H₂¹⁶O are expressed in the standard δ notation with respect to the VSMOW standard:

$$\delta = \frac{R_{\text{sample}}}{R_{\text{VSMOW}}} - 1 \quad (7)$$

where R stands for the ratio between water containing heavy isotopes (H₂¹⁷O, H₂¹⁸O or HDO) and H₂¹⁶O (note, for convenience, here and throughout the paper, we omit the factor of 10³ but the δ results are reported in ‰). It has been shown, however, that when dealing with high-precision ratios in multiple isotope systems a modified δ , hereafter designated δ' , should be preferred.²¹ This modified δ is defined as:

$$\delta' = \ln(\delta + 1) = \ln\left(\frac{R_{\text{sample}}}{R_{\text{VSMOW}}}\right) \quad (8)$$

In measurements of a large number of different meteoric water,^{3,6} it was found that, in a $\delta'^{17}\text{O}$ – $\delta'^{18}\text{O}$ plot, the data fall on a line whose slope is 0.528. Because this slope appears to be universal in meteoric water, we chose to use it as a reference slope.

The measured trend in meteoric water can be easily explained if it is assumed that condensation of vapor to liquid due to air cooling occurs in isotopic equilibrium. For a simple example we consider rainout and Rayleigh distillation of vapor that occurs with constant α_{eq} (α_{eq} stands for 17 or 18). Starting from atmospheric vapor with a given δ'^{O} , the δ'^{O} of the remaining fraction (f) of vapor after rainout is:

$$\delta'^{\text{O}} = \delta'^{\text{O}}_0 + (\alpha_{\text{eq}} - 1) \ln(f) \quad (9)$$

and the slope (γ) of meteoric water, which is derived from the vapor, is:

$$\gamma = \frac{(\delta'^{17}\text{O} - \delta'^{17}\text{O}_0)}{(\delta'^{18}\text{O} - \delta'^{18}\text{O}_0)} = \frac{(\alpha_{\text{eq}}^{17} - 1)}{(\alpha_{\text{eq}}^{18} - 1)} \quad (10)$$

Over the temperature range 0–30°C, ¹⁸ α_{eq} varies from 1.01172 to 1.00898 and ¹⁷ α_{eq} (= ¹⁸ α_{eq} ^{0.529}) from 1.00618 to 1.00474. In this case, (¹⁷ $\alpha_{\text{eq}} - 1$)/(¹⁸ $\alpha_{\text{eq}} - 1$) remains nearly constant and equals 0.528 ± 0.001.

In our previous study,¹⁴ we measured the $\delta^{17}\text{O}$ and $\delta^{18}\text{O}$ of meteoric water from different climate regions. When displayed in a $\delta^{17}\text{O}$ vs. $\delta^{18}\text{O}$ plot, all the meteoric water fall above a line with a slope of 0.528 that passes through VSMOW. These samples, therefore, have an excess of ¹⁷O with respect to ocean water. Accordingly, we define the ¹⁷O-excess as:

$$^{17}\text{O-excess} = \delta^{17}\text{O} - 0.528 \cdot \delta^{18}\text{O} \quad (11)$$

Because the magnitudes of the ¹⁷O-excess are very small, they are multiplied by 10⁶ and are reported in per meg with respect to VSMOW.

We emphasize that the ¹⁷O-excess does not result from mass-independent fractionations^{22,23} but from two mass-dependent processes of equilibrium and diffusion, in which the three oxygen isotope relationships are different. Figure 5 schematically explains the origin of the ¹⁷O-excess of meteoric water. According to Craig and Gordon,²⁴ the isotopic composition of vapor in the marine atmosphere is explained by liquid-vapor equilibrium near the ocean surface and then by vapor diffusion into under-saturated air. Because the $\delta^{17}\text{O}/\delta^{18}\text{O}$ ratio for diffusion is lower than for equilibrium, atmospheric vapor gains ¹⁷O-excess. Subsequent rainout proceeds with a slope of 0.528 (see above)

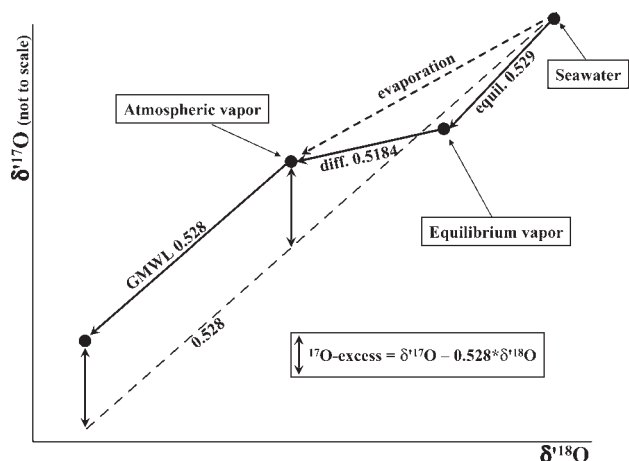


Figure 5. Schematic illustration showing the origin of ^{17}O -excess in meteoric water.

and thus does not affect the initial ^{17}O -excess gained above the ocean.

Following the approach of Merlivat and Jouzel,²⁵ we explain the ^{17}O -excess of marine vapor as a function of humidity and $^{18}\alpha_{\text{diff}}$. Let us consider a situation where there is local balance such that all the water lost by evaporation returns to the ocean as rain. In this case, the isotopic ratio of marine vapor equals that of the net evaporating flux, $R_A = R_E$. Using this condition, natural log transformation and rearrangement of Eqn. (1) we obtain:

$$\ln(R_E/R_W) = -\ln(^{18}\alpha_{\text{eq}}(^{18}\alpha_{\text{diff}}(1 - h_n) + h_n)) \quad (12)$$

Note that following Gat,²⁶ we use h_n instead of ordinary relative humidity (h), where h_n is the ratio of vapor concentration in the free air to the saturated concentration at the temperature and salinity of the sea surface. Using h_n is important in field situations where, unlike in laboratory experiments, the temperature of the air above the water surface may not be the same as that of the water. A simple example demonstrates this. Consider evaporation into air

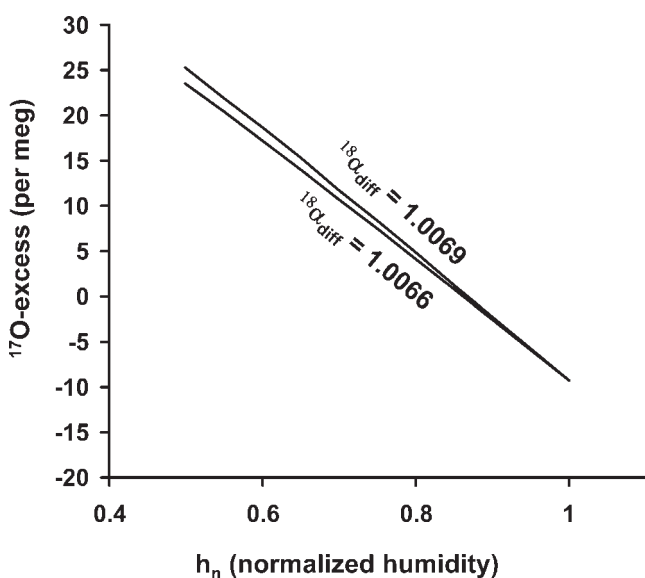


Figure 6. The dependence of ^{17}O -excess on normalized relative humidity and $^{18}\alpha_{\text{diff}}$.

cooler than the water surface. Even if the cooler air is saturated with vapor ($h = 1$) its vapor concentration will be less than in air in immediate contact with the water surface, and thus h_n will be less than 1 and there will be net sea-air vapor flux.

The term on the left of Eqn. (12) is δ' of atmospheric vapor with respect to local seawater (R_W), and the ^{17}O -excess of this vapor is then calculated as:

$$^{17}\text{O-excess} = -\ln(^{18}\alpha_{\text{eq}}^{0.529} (^{18}\alpha_{\text{diff}}^{0.518} (1 - h_n) + h_n)) + 0.528 \cdot \ln(^{18}\alpha_{\text{eq}} (^{18}\alpha_{\text{diff}} (1 - h) + h_n)) \quad (13)$$

We emphasize that, in natural situations, due to winds and subsequent turbulence, the magnitude of $^{18}\alpha_{\text{diff}}$ is much smaller than at stagnant conditions. Merlivat and Jouzel²⁵ used an approximation of $^{18}\alpha_{\text{diff}}$ as a function of wind speed. At low to moderate winds, when the water surface is smooth, $^{18}\alpha_{\text{diff}}$ equals 1.007, and this applies to about 95% of the ocean.²⁵ At higher wind speeds the surface becomes rough and $^{18}\alpha_{\text{diff}}$ varies between 1.003 and 1.005. In Fig. 6 we plot ^{17}O -excess as a function of h_n for $^{18}\alpha_{\text{diff}}$ of 1.0069 and 1.0066, corresponding to normal sea surface and to a combination of smooth and much rougher sea state, respectively. As can be seen, the ^{17}O -excess depends mainly on h_n , and, therefore, can be used to estimate past changes in humidity from aquifers containing fossil water as well as from ice cores.

CONCLUSIONS

We have presented high-precision measurements of diffusivity fractionations of water vapor in air. Using these results, we determined the ratio $\ln(^{17}\alpha_{\text{diff}})/\ln(^{18}\alpha_{\text{diff}})$ as 0.5185, which is significantly smaller than the corresponding ratio in vapor-liquid equilibrium (0.529), and gives rise to the ^{17}O -excess in meteoric water. The ^{17}O -excess is a robust indicator of evaporation conditions over the ocean, and a unique isotope property of water and ice that will be used in future studies of the hydrologic cycle.

Acknowledgements

We gratefully thank an anonymous reviewer for comments and excellent advice that significantly improved the manuscript. We also thank S. K. Bhattacharya for careful reading of the manuscript and useful suggestions. This research was supported by grant 188/03-13.0 from the Israel Science Foundation.

REFERENCES

- Gat JR. *Ann. Rev. Earth Planet. Sci.* 1996; **24**: 225.
- Luz B, Barkan E. *Science* 2000; **288**: 2028.
- Meijer HAJ, Li WJ. *Isotopes Environ. Health Stud.* 1998; **34**: 349.
- Angert A, Rachmilevitch S, Barkan E, Luz B. *Global Biogeochem. Cycles* 2003; **17**: 1030. DOI: 10.1029/2002GB001933.
- Angert A, Cappa CD, DePaolo DJ. *Geochim. Cosmochim. Acta* 2004; **68**: 3487.
- Barkan E, Luz B. *Rapid Commun. Mass Spectrom.* 2005; **19**: 3737.
- Ehhalt D, Knott K. *Tellus* 1965; **3**: 389.
- Criss RE. *Principles of Stable Isotope Distribution*. Oxford University Press: New York, 1999.
- Cappa CD, DePaolo DJ, Hendricks MB. *J. Geophys. Res.* 2003; **108D**: 4525.

10. Majoube M. *J. Chem. Phys.* 1971; **10**: 1423.
11. Horita J, Wesolowski DJ. *Geochim. Cosmochim. Acta* 1994; **58**: 3425.
12. Mook WG. *Environmental Isotopes in the Hydrological Cycle: Introduction*, vol. 1, Mook WG (ed). UNESCO, IAEA: Paris, 2000.
13. Merlivat L. *J. Chem. Phys.* 1978; **69**: 2864.
14. Landais A, Barkan E, Yakir D, Luz B. *Geochim. Cosmochim. Acta* 2006; **70**: 4105.
15. Fang G, Ward CA. *Phys. Rev.* 1999; **59**: 417.
16. Paulson CA, Parker TW. *J. Geophys. Res.* 1972; **77**: 491.
17. Marrero TR, Mason EA. *J. Phys. Chem. Reference Data* 1972; **1**: 3.
18. Hirschfelder JO, Curtiss CF, Bird RB. *Molecular Theory of Gases and Liquids*. John Wiley: New York, 1964.
19. Pfeilsticker K, Lotter A, Peters C, Bösch H. *Science* 2003; **300**: 2078.
20. Vaida V, Headrick JE. *J. Phys. Chem. A* 2000; **104**: 5401.
21. Hulston JR, Thode HG. *J. Geophys. Res.* 1965; **70**: 3475.
22. Thiemens MH. *Science* 1999; **283**: 341.
23. Luz B, Barkan E, Bender ML, Thiemens MH, Boering KA. *Nature* 1999; **400**: 547.
24. Craig H, Gordon LI. *Stable Isotope in Oceanographic Studies and Paleotemperatures*. V. Lischi e Figli: Pisa, 1965; 122.
25. Merlivat L, Jouzel J. *J. Geophys. Res.* 1979; **84**: 5029.
26. Gat JR. *Earth Planet. Sci. Lett.* 1984; **71**: 361.
27. Ludwig K. *A Geochronological Toolkit for Microsoft Excel*, Berkeley Geochronology Center: Berkeley, 2003, 71. Available: <http://www.bgc.org/klprogramm.html>.